Reduced boron diffusion under interstitial injection in fluorine implanted silicon

M. N. Kham,[a] I. Matko,[b] B. Chenevier,[b] and P. Ashburn
School of Electronics and Computer Science, University of Southampton, Southampton SO17 1BJ, United Kingdom

(Received 2 August 2007; accepted 22 October 2007; published online 12 December 2007)

Point defect injection studies are performed to investigate how fluorine implantation influences the diffusion of boron marker layers in both the vacancy-rich and interstitial-rich regions of the fluorine damage profile. A 185 keV, 2.3×10^{15} cm^{-2} F^+ implant is made into silicon samples containing multiple boron marker layers and rapid thermal annealing is performed at 1000 °C for times of 15–120 s. The boron and fluorine profiles are characterized by secondary ion mass spectroscopy and the defect structures by transmission electron microscopy (TEM). Fluorine implanted samples surprisingly show less boron diffusion under interstitial injection than those under inert anneal. This effect is particularly noticeable for boron marker layers located in the interstitial-rich region of the fluorine damage profile and for short anneal times (15 s). TEM images show a band of dislocation loops around the range of the fluorine implant and the density of dislocation loops is lower under interstitial injection than under inert anneal. It is proposed that interstitial injection accelerates the evolution of interstitial defects into dislocation loops, thereby giving transient enhanced boron diffusion over a shorter period of time. The effect of the fluorine implant on boron diffusion is found to be the opposite for boron marker layers in the interstitial-rich and vacancy-rich regions of the fluorine damage profile. For marker layers in the interstitial-rich region of the fluorine damage profile, the boron diffusion coefficient decreases with anneal time, as is typically seen for transient enhanced diffusion. The boron diffusion under interstitial injection is enhanced by the fluorine implant at short anneal times but suppressed at longer anneal times. It is proposed that this behavior is due to trapping of interstitials at the dislocation loops introduced by the fluorine implant. For boron marker layers in the vacancy-rich region of the fluorine damage profile, suppression of boron diffusion is seen for short anneals and then increased diffusion after a critical time, which is longer for inert anneal than interstitial injection. This behavior is explained by the annealing of vacancy-fluorine clusters, which anneal quicker under interstitial injection because the injected interstitials annihilate vacancies in the clusters. © *2007 American Institute of Physics*.
[DOI: 10.1063/1.2822465]

INTRODUCTION

Over the past few years, there has been considerable interest in the behavior of fluorine in silicon for application in bipolar and metal-oxide-semiconductor (MOS) devices. This interest has been motivated by the effect of fluorine in totally suppressing boron transient enhanced diffusion[1–9] (TED) and also in reducing boron thermal diffusion[7,8] in silicon. When applied to complementary MOS technology, fluorine implantation has been shown to improve the threshold voltage roll-off in *p*-channel transistors[10] and has been used to produce a supersharp halo profile in *n*-channel transistors.[11] The recent application of fluorine implantation to silicon bipolar technology has delivered a record f_T of 110 GHz.[12]

Although the effect of fluorine is well documented in the literature, its mechanism in suppressing boron diffusion is still under research. Initial work[5] suggested that the suppression of boron diffusion by fluorine was due to chemical effect of the fluorine. However, later work on fluorine implantation into crystalline silicon showed that the suppression of boron thermal diffusion by fluorine correlated with the presence of a shallow fluorine secondary ion mass spectroscopy (SIMS) peak at approximately half the range of the fluorine implant.[7,8] The shallow fluorine peak was attributed to vacancy-fluorine (V-F) clusters[7,8] and point defect injection experiments have since been performed that confirm this interpretation.[13,14] Positron annihilation spectroscopy has also directly confirmed the presence of V-F clusters in fluorine implanted silicon.[15] Recent work on fluorine implantation into preamorphized silicon has also suggested that V-F clusters are responsible for the suppression of boron transient enhanced diffusion.[9] However, contradictory results have also been reported,[16] which indicate that for fluorine implants into crystalline SiGe, suppression of boron TED is also obtained even when the shallow SIMS peak due to V-F clusters is not present. These results suggest that mechanisms other than V-F clusters can contribute to the suppression of boron diffusion in Si and SiGe.

In this paper, point defect injection studies are performed to investigate how fluorine implantation influences the diffu-

[a]Electronic mail: mnk03r@ecs.soton.ac.uk.
[b]Also at Laboratoire des Matériaux et du Génie Physique, BP 257–INPGrenoble Minatec-3 parvis Louis Néel-38016 Grenoble, France.

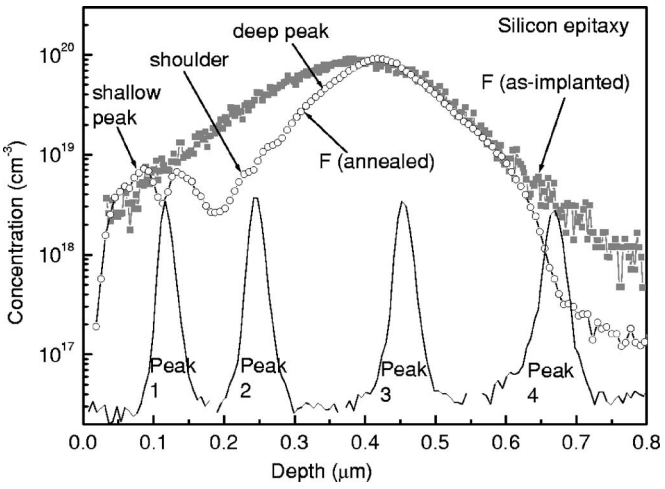

FIG. 1. SIMS profiles of boron marker layers after growth showing the location of the four boron peaks with respect to the fluorine profiles after implant and anneal.

sion of boron marker layers in both the vacancy-rich and interstitial-rich regions of the fluorine damage profile. Fluorine implanted samples show less boron diffusion under interstitial injection than under inert anneal, particularly when boron marker layers are located in the interstitial-rich region of the fluorine damage profile and when the anneal time is short. This is a surprising result as it is opposite to the accepted effect of interstitials on boron diffusion. Furthermore, the effect of fluorine on boron diffusion is found to be the opposite for boron marker layers in the interstitial-rich and vacancy-rich regions of the fluorine damage profile. For boron marker layers in the interstitial-rich region, boron diffusion suppression is seen for long anneals under interstitial injection, whereas for marker layers in the vacancy-rich region, it is seen for short anneals. The results of detailed SIMS and transmission electron microscopy (TEM) experiments are reported and the results are explained by the effect of dislocation loops on the boron diffusion in the interstitial-rich region of the fluorine damage profile and by vacancy-fluorine clusters in the vacancy-rich region.

EXPERIMENTAL PROCEDURE

Boron diffusion in different regions of the fluorine implant damage profile was investigated using four boron marker layers grown using low pressure chemical vapour deposition (LPCVD). The four boron marker layers were located at depths of 0.12, 0.24, 0.45, and 0.67 μm as shown in Fig. 1. Each marker layer has a peak boron concentration of approximately 3×10^{18} cm^{-3} and width of ~30 nm at a concentration of 1×10^{18} cm^{-3}. Peak 1 was chosen to lie in the vacancy-rich region of the fluorine damage profile and peaks 3 and 4 in the interstitial-rich region.

A 185 keV, 2.3×10^{15} cm^{-2} F$^+$ was implanted into half of each wafer using a photoresist half-mask. Both the implanted and nonimplanted sections were divided again into three parts for defect injection study. The first part was covered with LPCVD SiO_2 and Si_3N_4 layers for inert anneal and the second part was uncovered for interstitial injection (I-inj). The SiO_2 layer was ~100 nm thick and was deposited

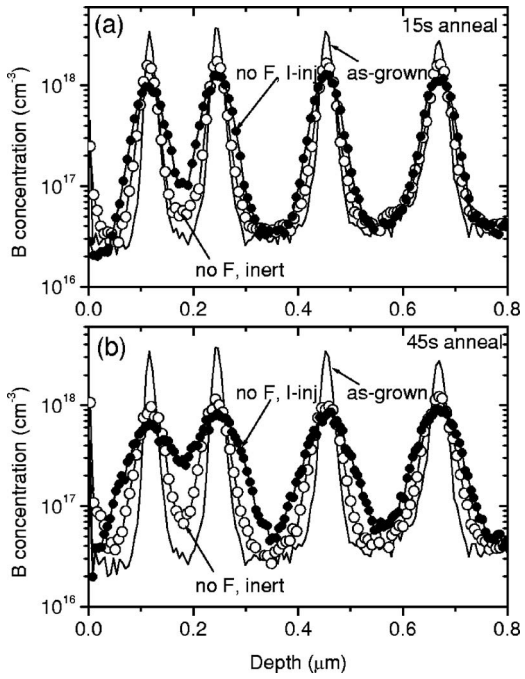

FIG. 2. SIMS profiles of boron marker layers after anneal at 1000 °C under interstitial injection and inert conditions. The as-grown boron profile is shown for comparison. (a) Shows the boron profiles after a 15 s anneal and (b) shows the profiles after a 45 s anneal.

at 400 °C and the Si_3N_4 layer was ~130 nm thick and was deposited at 300 °C. This method of selective point defect injection has been successfully applied to boron and arsenic diffusions in Si and SiGe,[17,18] and further details can be found in Ref. 13. The wafers were then cut into 1×1 cm^2 pieces and annealed at 1000 °C for 10–120 s in an oxygen atmosphere. The SiO_2 and Si_3N_4 layers were stripped before the SIMS analysis was performed. TEM analysis was also performed on some samples. The thin foils were prepared using a classical preparation method including first a mechanical polishing followed by ion milling. The TEM observations have been performed on JEM 2010 (200 kV) and JEM 3010 (300 kV) electron microscopes.

RESULTS

Figure 2(a) shows the effect of point defect injection on boron diffusion in unimplanted samples. Boron SIMS profiles are shown for samples annealed for 15 s at 1000 °C under inert and interstitial injection conditions. The as-grown boron profile is also shown for reference. It can be seen that boron diffusion under interstitial injection is greater than that under inert anneal for all four peaks. This result is as expected, since it is well known that boron diffusion is mediated by interstitials and hence interstitial injection from the surface should enhance boron diffusion. Similar behavior is also observed for longer anneal times, as illustrated in Fig. 2(b) for a 45 s anneal at 1000 °C.

Figure 3(a) shows the effect of point defect injection on boron diffusion for samples given a prior 185 keV, 2.3×10^{15} cm^{-2} F$^+$ implant. Boron SIMS profiles are shown for fluorine implanted samples annealed at 1000 °C under inert and interstitial injection conditions for 15 s. The as-grown

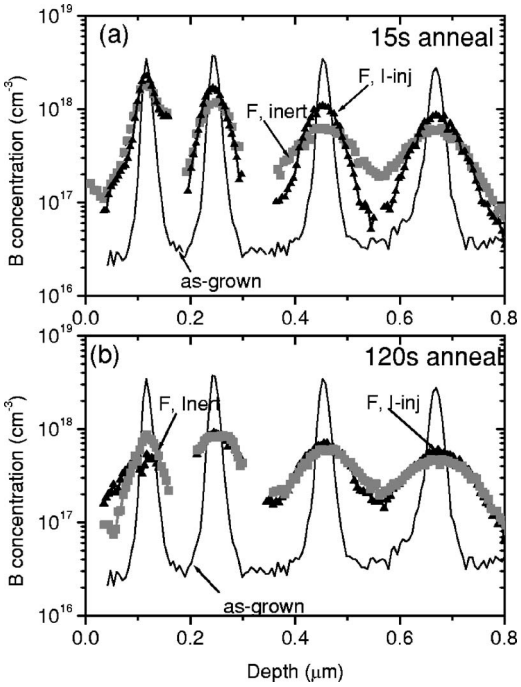

FIG. 3. SIMS profiles of boron marker layers after a 185 keV, 2.3×10^{15} cm^{-2} F^+ implant and an anneal at 1000 °C under interstitial injection and inert conditions. The as-grown boron profile is shown for comparison. (a) Shows the boron profiles after a 15 s anneal and (b) shows the profiles after a 120 s anneal.

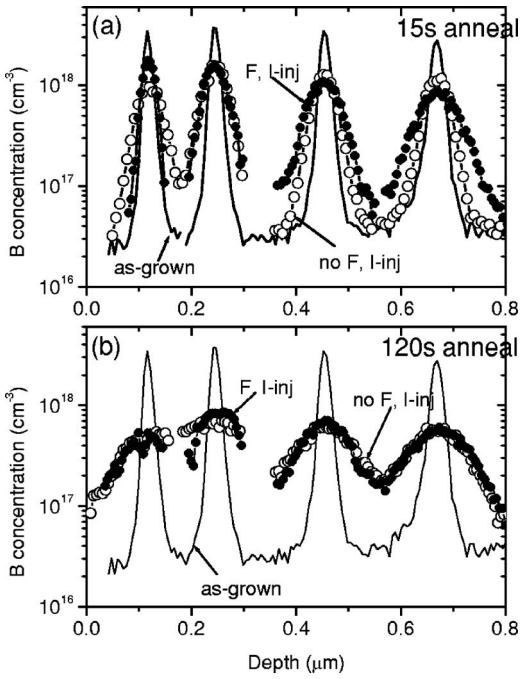

FIG. 4. Comparison of boron SIMS profiles in fluorine implanted (185 keV, 2.3×10^{15} cm^{-2}) and unimplanted samples annealed at 1000 °C under interstitial injection. The as-grown boron profile is shown for comparison. (a) Shows the boron profiles after a 15 s anneal and (b) shows the profiles after a 120 s anneal.

boron profile is also shown for reference. Interestingly for the two deepest peaks, the boron diffusion under interstitial injection is significantly less than that under inert anneal. This is the opposite result to that obtained for the unimplanted samples in Fig. 2 and is very surprising, since boron diffusion is mediated by interstitials and hence it would be expected that the boron diffusion would be greater under interstitial injection than under inert anneal. For the two shallowest peaks, the boron diffusion under interstitial injection is again less than that seen under inert anneal, but the difference is small.

Figure 3(b) shows the effect of point defect injection on boron diffusion for F^+ implanted samples annealed for 120 s at 1000 °C under inert and interstitial injection conditions. The amount of diffusion in this case is much larger than that in Fig. 3(a) but, nevertheless, for the two deepest peaks, the amount of boron diffusion under interstitial injection is slightly less than that under inert anneal. However, for the shallowest peak, the opposite trend is seen, with less diffusion under inert anneal than under interstitial injection.

Figure 4(a) shows the effect of a fluorine implant on boron diffusion after an anneal of 15 s at 1000 °C under interstitial injection. For peak 1, the fluorine implant has given a significant reduction in the boron diffusion, whereas for peaks 3 and 4, the fluorine implant has given a small increase in the amount of boron diffusion. For peak 2, the behavior is intermediate and the fluorine implant has had little effect on the boron profile. For comparison, Fig. 4(b) shows the effect of a fluorine implant on boron diffusion after a longer anneal of 120 s at 1000 °C under interstitial injection. In this case the boron diffusion is similar in the fluorine implanted and unimplanted samples for all four boron peaks.

To fully characterize the boron diffusion under inert anneal and interstitial injections for all anneal times, the boron profiles were simulated and values of diffusion coefficient extracted. Figure 5 shows the values of boron diffusion coefficient as a function of anneal time for boron peaks 1 and 3, which are typical of the behavior in the vacancy-rich and interstitial-rich regions of the fluorine damage profiles, respectively. Results are shown for the time intervals 0–15, 15–45, and 45–120 s. For the unimplanted samples given an inert anneal (no F, Inert), the average diffusion coefficient is constant for all three boron marker layers, with a value of 3.1×10^{-14} cm^2/s which is slightly larger than the value of 1.53×10^{-14} cm^2/s reported by Fair for intrinsic boron diffusion.[19] The diffusion coefficient under interstitial injection (no F, I-Inj) also shows a constant value of 1.1×10^{-13} cm^2/s for all four boron marker layers and for all anneal times. This indicates that interstitials are injected into the silicon at a constant rate for oxidation times up to 120 s.

For the fluorine implanted samples, Fig. 5(a) shows the boron diffusion coefficient as a function of time for peak 1, which is located in the vacancy-rich region of the fluorine damage profile. Under interstitial injection, the boron diffusion coefficient in the fluorine implanted samples (F, I-Inj) is small in the 0–15 s time interval and equal to that for the unimplanted sample given an inert anneal (no F, Inert). A similar low value of boron diffusion coefficient is obtained for fluorine implanted samples annealed under inert conditions (F, Inert). This indicates that for short anneals, the fluorine implant suppresses the enhanced boron diffusion arising

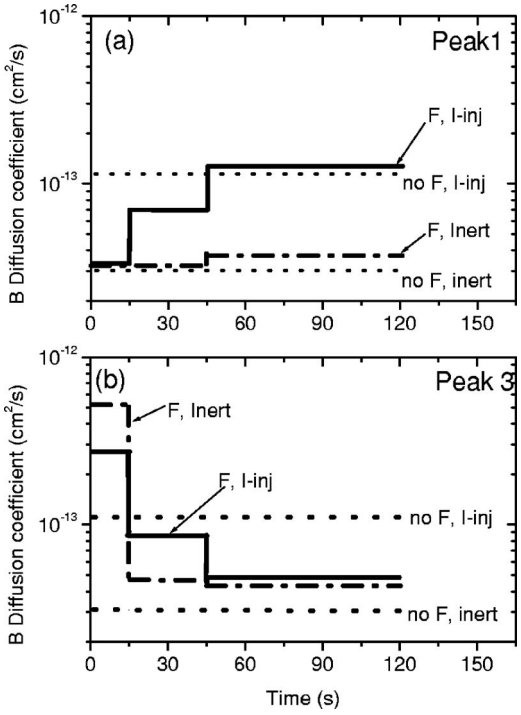

FIG. 5. Boron diffusion coefficient as a function of anneal time for fluorine implanted (185 keV, 2.3×10^{15} cm^{-2}) and unimplanted samples annealed at 1000 °C under interstitial injection and inert conditions. (a) Shows the values of boron diffusion coefficient for a boron marker layer located in the vacancy-rich region of the fluorine damage profile and (b) for a marker layer located in the interstitial-rich region of the damage profile.

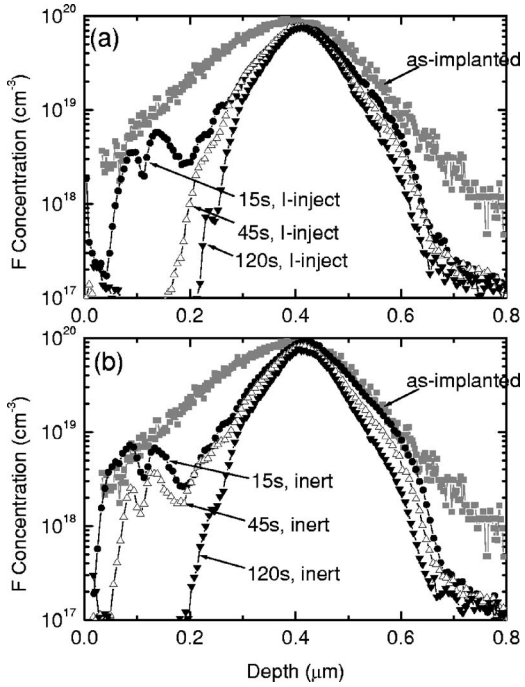

FIG. 6. Fluorine SIMS profiles for samples implanted with 185 keV, 2.3×10^{15} cm^{-2} F$^+$ and annealed for different times at 1000 °C under (a) interstitial injection conditions and (b) inert conditions. An as-implanted fluorine profile is shown for comparison.

from interstitials injected from the surface. For the 45–120 s time interval, a high value of boron diffusion coefficient is obtained in the fluorine implanted samples annealed under interstitial injection (F, I-Inj) and this value is close to that for the unimplanted sample (no F, I-Inj). This indicates that for long anneals, the fluorine implant is not effective in suppressing the enhanced boron diffusion due to interstitials injected from the surface. In contrast, for the fluorine implanted sample annealed under inert conditions (F, Inert), a low value of boron diffusion coefficient is obtained, slightly larger than that obtained for the equivalent unimplanted sample (no F, Inert).

For the fluorine implanted samples, Fig. 5(b) shows the boron diffusion coefficient as a function of time for peak 3, which is located in the interstitial-rich region of the fluorine damage profile. For the 0–15 s time period, very high values of boron diffusion coefficient are obtained for the fluorine implanted samples under both interstitial injection and inert anneal. For the 45–120 s time interval, lower values of boron diffusion coefficient are obtained and the value under interstitial injection, is similar to that under inert anneal. However, under interstitial injection, the fluorine implanted sample (F, I-Inj) has a significantly lower diffusion coefficient than the unimplanted control (no F, I-Inj). This indicates that fluorine suppresses enhanced boron diffusion arising from interstitial injection even when the boron marker layer is in the interstitial rich region of the fluorine damage profile.

To investigate the cause of the different boron diffusion behaviors under interstitial injection and inert anneal, Fig. 6 shows fluorine SIMS profiles for a range of anneal times (15, 45, and 120 s) for each injection condition. For the sample given a 15 s anneal under interstitial injection, Fig. 6(a) shows that a shallow double fluorine peak is present at a depth of about 0.03–0.2 μm. The position of the dip between the two fluorine peaks coincides with the position of the peak 1 boron marker layer. This shallow fluorine peak has largely disappeared after interstitial injection for 45 s. Figure 6(a) also shows the presence of a deep fluorine peak at a depth of approximately 0.41 μm. The peak concentration of this deep fluorine peak decreases slightly with increasing anneal time under interstitial injection and also becomes narrower.

For comparison, Fig. 6(b) shows the evolution of the fluorine profiles under inert anneal for anneals of 15, 45, and 120 s at 1000 °C. The major difference between this fluorine profile and that in Fig. 6(a) is that the shallow fluorine peak is present after a 45 s inert anneal but is absent after a 45 s anneal under interstitial injection, as can be seen by comparing Figs. 6(a) and 6(b). Furthermore for the 15 s anneal, the fluorine concentration in the shallow peak at the depth of 0.1 μm is higher under inert anneal (7×10^{18} cm^{-3}) than that under interstitial injection (3.5×10^{18} cm^{-3}). The behavior of the deep fluorine peak under inert anneal is similar to that under interstitial injection.

To better understand the fluorine profiles, Fig. 7 compares cross-section TEM images of samples annealed at 1000 °C for 120 s under inert anneal (a) and interstitial injection (b). For the sample given an inert anneal, Fig. 7(a) shows a dense band of dislocation loops extending from a depth of about 0.34–0.7 μm ($0.9R_p$ to $1.8R_p$). A comparison with the SIMS profile in Fig. 6(b) shows that this band of

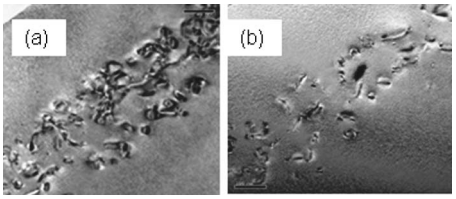

FIG. 7. Cross-section TEM micrographs (bright field) of samples implanted with 185 keV, 2.3×10^{15} cm^{-2} F^+ and annealed for 120 s at 1000 °C under (a) inert conditions and (b) interstitial injection from the surface. The magnification bar is 100 nm in both cases.

loops corresponds approximately to the deep fluorine peak on the SIMS profile ($0.7R_p$ to $2R_p$). There is no evidence of defects shallower than 0.34 μm, which corresponds to the depth of the shallow fluorine peak (0–0.2 μm). For the sample heated under interstitial injection, Fig. 7(b) shows a sparse band of dislocation loops at a similar depth to those in Fig. 7(a). Again there is no evidence of defects in the vicinity of the shallow fluorine peak. The typical size of the dislocation loops ranges between 15 and 100 nm.

Figure 8 shows plan-view TEM images of samples annealed at 1000 °C for 120 s under inert anneal (a) and interstitial injection (b). These plan-view images show a similar trend to the cross-section images in Fig. 7, namely, a dense network of dislocation loops in the sample given an inert anneal and a sparser network in the sample given an anneal under interstitial injection.

From the various TEM observations, it is possible to show that the loop density per area unit in the inert anneal sample is close to 2.0×10^{10} cm^{-2}. In the sample annealed under interstitial injection, the loop density is approximately 30% lower.

DISCUSSION

It is now well established that boron TED is caused by implantation damage and occurs during the initial phase of annealing when a large supersaturation of interstitials is present.[20] The interstitials evolve into interstitial clusters, {311} defects, and eventually dislocation loops,[21] at which point the transient enhanced diffusion stops. The decrease in boron diffusion coefficient with increasing anneal time seen for boron peak 3 in Fig. 5(b) can therefore be explained by TED arising from damage created by the fluorine implant. Peak 3 is in the interstitial-rich region of the fluorine damage profile, where the defects responsible for TED are located and hence these defects would directly affect the diffusion of boron peak 3. Figure 5(b) shows that the enhanced boron diffusion is primarily seen in the 0–15 s time period, which implies that majority of the TED occurs in the first 15 s of the anneal. This conclusion is consistent with the results of a study by Michel *et al.*,[22] who showed that boron TED ends after ~15 s at 950 °C.

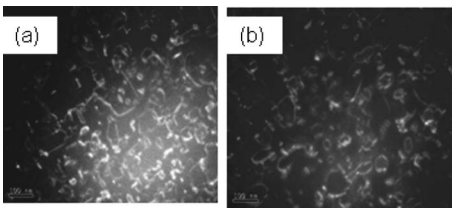

FIG. 8. Plan-view TEM micrographs (weak beam dark field, $\mathbf{B}=[0\ 0\ 1]$, $\mathbf{g}=\langle 400\rangle$) of samples implanted with 185 keV, 2.3×10^{15} cm^{-2} F^+ and annealed for 120 s at 1000 °C under (a) inert conditions and (b) interstitial injection from the surface. The magnification bar is 100 nm in both cases.

The injection of interstitials from the surface has a similar effect in enhancing boron diffusion as implantation-induced interstitials. This can be clearly seen in the results for the unimplanted samples in Fig. 5, where the boron-diffusion coefficient under interstitial injection (1.1×10^{-13} cm^2/s) is a factor of 3.5 larger than that under inert anneal (3.1×10^{-14} cm^2/s). Our results are in accordance with the linear oxidation expected for short oxidation times, since the surface reaction is the rate-limiting factor.[23] This enhancement, which is independent of the anneal time, is in agreement with previous reports by Skarlatos *et al.*[24] and Park *et al.*[25] who used boron marker layers and dry oxidation at 900 °C for times of 30 min to 4 h. The boron diffusion coefficient under interstitial injection was a factor of 3.3 higher than that under inert anneal.

In the fluorine implanted samples, the lower value of boron diffusion coefficient seen in the 0–15 s time interval under interstitial injection than that under inert anneal [Figs. 3(a) and 5(b)] is a surprising result. Boron diffusion is mediated by interstitials and, hence, at first sight, it would be expected that the boron diffusion would be greater under interstitial injection than under inert anneal. This result can be interpreted using the TEM images in Figs. 7 and 8, which show fewer dislocation loops under interstitial injection than under inert anneal. As discussed above, the evolution of free interstitials during anneal follows the sequence of cluster formation, transformation into {311} defects and, finally, dislocation loop formation. The TEM images in Figs. 7 and 8 suggest that this sequence is accelerated under interstitial injection. Once formed, dislocation loops follow an Ostwald ripening process,[26] in which small dislocation loops lose interstitials to larger loops. This leads to a decrease in the density of dislocation loops with increasing anneal time and an increase in the loop size. The lower dislocation loop density in Figs. 7 and 8 under interstitial injection therefore provides evidence for accelerated Ostwald ripening. This acceleration of defect evolution would be expected to give earlier transformation of {311} defects into dislocation loops and hence enhanced boron diffusion would be seen over a shorter period of time. This mechanism would explain the smaller value of boron diffusion coefficient in Fig. 5(b) under interstitial injection than under inert anneal in the 0–15 s time interval.

In the fluorine implanted samples annealed for 45–120 s under interstitial injection, Fig. 5(b) shows that the boron diffusion coefficient in the F implanted sample (5×10^{-14} cm^{-2}) is significantly lower than that in the unimplanted control sample (1.1×10^{-13} cm^{-2}). This indicates that fluorine suppresses boron diffusion even when the boron marker layer is located in the interstitial-rich region of the fluorine damage profile. There are no dislocation loops in the unimplanted samples, so this result implies that the dislocation loops in the fluorine implanted samples soak up free

interstitials injected from the surface. If the majority of interstitials were tied up in the dislocation loops so that the interstitial flux in the dislocation band was small, then the boron diffusion in the fluorine implanted samples might well be lower than that in the unimplanted control samples, where there would be considerable flux of interstitials from the surface. Dislocation loops are well known to be good sinks for interstitials.[24,25] For example, Park *et al.*[25] reported an ~50% suppression of boron oxidation enhanced diffusion by dislocation loops during oxidizing anneal at 900 °C for 30 min. This mechanism is also consistent with the results of El Mubarek *et al.*,[8] who attributed suppression of boron transient enhanced diffusion to the retention of interstitials in dislocation loops.

The results for peak 1, which lies in the vacancy-rich region of the fluorine damage profile, show the opposite trend to those for peak 3, which lies in the interstitial-rich region of the damage profile. This can be clearly seen in Fig. 5, where the boron diffusion coefficient increases with anneal time for peak 1 but decreases for peak 3. It is now generally agreed that following an implant, vacancies are the dominating defect species in a layer between the surface and approximately R_p, while self-interstitials are mainly observed around R_p and beyond. El Mubarek *et al.*[7] proposed that the shallow fluorine peak, which is responsible for a reduction in boron thermal diffusion, was due to vacancy-fluorine clusters. The behavior of the shallow peak observed in Fig. 6 supports this idea. An excellent correlation is obtained between the fluorine SIMS profiles in Fig. 6 and the boron diffusion coefficients for boron peak 1 in Fig. 5(a). For the fluorine implanted sample under interstitial injection, the rise of the boron diffusion coefficient for the 15–45 s time period coincides with the elimination of the shallow fluorine peak in Fig. 6(a) after a 45 s anneal. Similarly, for the fluorine implanted sample under inert anneal, the rise of the boron diffusion coefficient for the 45–120 s time period coincides with the elimination of the shallow fluorine peak after a 120 s anneal in Fig. 6(b). The earlier elimination of the shallow fluorine peak under interstitial injection is consistent with the annihilation of V-F clusters by the interstitials injected from the surface.

CONCLUSIONS

Point defect injection studies have been performed to investigate how fluorine implantation influences the diffusion of boron marker layers in both the vacancy-rich and interstitial-rich regions of a fluorine damage profile. Contrary to the generally accepted behavior, fluorine implanted samples show less boron diffusion under interstitial injection than under inert anneal. This surprising result is explained by the accelerated Ostwald ripening of dislocation loops under interstitial injection, as confirmed by TEM images. The effect of the fluorine implant on boron diffusion is found to be the opposite for boron marker layers in the interstitial-rich and vacancy-rich regions of the fluorine damage profile. For boron marker layers in the interstitial-rich region, the boron diffusion coefficient decreases with increasing anneal time. This trend is explained by TED arising from damage created by the fluorine implant. For long anneals under interstitial injection, suppression of boron diffusion is observed in fluorine implanted samples compared with unimplanted controls. This indicates that fluorine is able to suppress boron diffusion even when the boron marker layer is in the interstitial-rich region of the fluorine damage profile and is explained by the capture of injected interstitials by the dislocation loops. For boron marker layers in the vacancy-rich region, suppression of the boron diffusion coefficient is observed for short anneals, followed by an increase at longer anneal times. This behavior is explained by the suppression of boron diffusion by vacancy-fluorine clusters at short anneal times, followed by the dissolution of the clusters at longer anneal times. The vacancy-fluorine clusters survive longer during inert anneal than during interstitial injection because the injected interstitials tend to annihilate vacancies in the clusters.

[1] R. G. Wilson, J. Appl. Phys. **54**, 6879 (1983).
[2] K. Ohyu, T. Itoga, and N. Natsuaki, Jpn. J. Appl. Phys., Part 1 **29**, 457 (1990).
[3] D. Fan, J. M. Parks, and R. J. Jaccodine, Appl. Phys. Lett. **59**, 1212 (1991).
[4] L. Y. Krasnobaev, N. M. Omelyanovskaya, and V. V. Makarov, J. Appl. Phys. **74**, 6020 (1993).
[5] J. Liu, D. F. Downey, K. S. Jones, and E. Ishida, *Proceedings of the International Conference on Ion Implantation Technology*, Kyoto, Japan, 22–26 June 1998, edited by J. Matsuo, G. Takaoka, and I. Yamada (IEEE, Piscataway, NJ, 1999), Vol. 2, p. 951.
[6] T. S. Shano, R. Kim, T. Hirose, Y. Furuta, H. Tsuji, M. Furuhashi, and K. Taniguchi, Tech. Dig. - Int. Electron Devices Meet. **2001**, 37.4.1.
[7] H. A. W. El Mubarek and P. Ashburn, Appl. Phys. Lett. **83**, 4134 (2003).
[8] H. A. W. El Mubarek, J. M. Bonar, G. D. Dilliway, M. Karunaratne, A. F. Willoughby, Y. Wang, P. L. F. Hemment, R. Price, J. Zhang, P. Ward, and P. Ashburn, J. Appl. Phys. **96**, 4114 (2004).
[9] G. Impellizzeri, S. Mirabella, F. Priolo, E. Napolitana, and A. Carnera, J. Appl. Phys. **99**, 103510 (2006).
[10] H. Fukutome, Y. Momiyama, H. Nakao, T. Aoyama, and H. Arimoto, Tech. Dig. - Int. Electron Devices Meet. **2003**, 485.
[11] K. Liu, J. Wu, J. Chen, and A. Jain, IEEE Electron Device Lett. **24**, 180 (2003).
[12] M. N. Kham, H. A. W. El Mubarek, J. M. Bonar, P. Ward, L. Fiore, R. Petralia, C. Alemanni, A. Messina, and P. Ashburn, IEEE Trans. Electron Devices **53**, 545 (2006).
[13] M. N. Kham, H. A. W. El Mubarek, J. M. Bonar, and P. Ashburn, Appl. Phys. Lett. **87**, 011902 (2005).
[14] M. N. Kham, H. A. W. El Mubarek, J. M. Bonar, D. Chivers, and P. Ashburn, Nucl. Instrum. Methods Phys. Res. B **253**, 100 (2006).
[15] X. D. Pi, C. P. Burrows, and P. G. Coleman, Phys. Rev. Lett. **90**, 155901 (2003).
[16] H. A. W. El Mubarek, M. Karunaratne, J. M. Bonar, G. D. Dilliway, Y. Wang, P. L. F. Hemment, A. F. Willoughby, and P. Ashburn, IEEE Trans. Electron Devices **52**, 518 (2005).
[17] J. M. Bonar, B. M. McGregor, N. E. B. Cowern, A. H. Dan, G. A. Cooke, and A. F. W. Willoughby, *Si Front-End Processing Physics and Technology of Dopant-Defect Interactions II*, MRS Symposia Proceedings No. 610 (Materials Research Society, Pittsburgh, 2001), p. B.4.9.1.
[18] S. Uppal, A. F. W. Willoughby, J. M. Bonar, and J. Zhang, Appl. Phys. Lett. **85**, 552 (2004).
[19] R. B. Fair, in *Impurity Doping*, edited by F. F. Y. Wang (North-Holland, Amsterdam, 1981), Chap. 7, p. 315.
[20] H. G. Z. Huizing, C. C. G. Visser, N. E. B. Cowern, P. A. Stolk, and R. C. M. de Kriof, Appl. Phys. Lett. **69**, 1211 (1996).
[21] A. Claverie, L. F. Giles, M. Omri, B. de Mauduit, G. Ben Assayag, and D. Mathiot, Nucl. Instrum. Methods Phys. Res. B **147**, 1 (1999).
[22] A. E. Michel, W. Raush, P. A. Ronsheim, and R. H. Kastl, Appl. Phys. Lett. **50**, 416 (1987).
[23] S. M. Sze, *Semiconductor Devices, Physics and Technology*, 2nd ed.

(Wiley, New York, 2002), pp. 370–378.
[24]D. Skarlatos, D. Tsoukalas, L. F. Giles, and A. Claverie, J. Appl. Phys. **87**, 1103 (2000).
[25]H. Park, H. Robinson, K. S. Jones, and M. E. Law, Appl. Phys. Lett. **65**, 436 (1994).
[26]N. E. B. Cowern, B. Colombeau, E. Lampin, F. Cristiano, A. Claverie, Y. Lamrani, R. Duffy, V. Venezia, A. Heringa, C. C. Wang, and C. Zechner, *CMOS Front-End Materals and Process Technology*, MRS Symposia Proceedings No. 765 (Materials Research Society, Pittsburgh, 2003), p. D6.8.1.